Raman Spectra of TiO_2, MgF_2, ZnF_2, FeF_2, and MnF_2

S. P. S. Porto, P. A. Fleury, and T. C. Damen
Bell Telephone Laboratories, Murray Hill, New Jersey
(Received 11 August 1966)

First-order Raman spectra have been measured at room temperature in five materials of the D_{4h} point group: TiO_2, MgF_2, ZnF_2, FeF_2 and MnF_2. The experiments utilized an argon laser light source and photoelectric detection. The four Raman-active phonon frequencies, predicted by group theory to have symmetries A_{1g}, B_{1g}, B_{2g}, and E_g, were observed and classified in each material. Each spectrum exhibited strong lines of A_{1g} and E_g symmetries, a weak high-frequency line of B_{2g} symmetry, and a very sharp B_{1g} line at quite low frequency (less than 100 cm^{-1} in all the materials except TiO_2).

INTRODUCTION

THE phonon frequencies and symmetries in the metal fluorides ZnF_2, MgF_2, MnF_2, and FeF_2 which have the rutile (TiO_2) structure, D_{4h}, are of interest for several reasons. For example, "phonon-terminated" laser action has been reported recently in doped MgF_2 and ZnF_2.[1] Also several transition metal fluorides, such as MnF_2 and FeF_2, exhibit antiferromagnetism at low temperatures. In these cases a detailed knowledge of the phonon spectra is desired from the viewpoint of possible phonon-magnon interactions. The infrared-active phonons have been observed in TiO_2,[2] MgF_2 and ZnF_2,[3] and FeF_2.[4] Raman spectra have been reported for TiO_2 [5–7] and MgF_2.[8,9] However in only one of the Raman experiments was a laser source used, so that polarization data were often lacking or unreliable. In the lone laser study[9] the crystal was not fully oriented so that complete phonon symmetry assignments could not be made.

In all the experiments described here a linearly polarized laser light source and completely oriented single-crystal samples have made possible unambiguous determination of the symmetries as well as the frequencies for the Raman-active phonons.

In the next section of this paper, we discuss briefly the experimental details, including the possibly misleading effects of improper crystal orientation. In the final section the results of our Raman experiments are presented and discussed in terms of both infrared and, where applicable, other Raman scattering results. Our conclusions concerning TiO_2 disagree with all but one of the previously reported Raman experiments, that of Krishnamurti. The earlier reports[8,9] of Raman spectra in MgF_2 not only disagree with each other, but with our results as well.

EXPERIMENTAL

To obtain the Raman spectra, we use ~75 mW of linearly polarized, 4880-Å light from an argon ion laser as the exciting source. Light scattered through 90° is passed through a double Czerny Turner spectrometer and detected photoelectrically. All samples used are oriented single crystals. All designations of the Raman tensor elements are referred to the crystal axes of the unit cell shown in Fig. 1. There are two molecules (six atoms) in the unit cell, implying a total of 15 vibrational modes. These modes have the irreducible representation[10]

$$1A_{1g}+1A_{2g}+1A_{2u}+1B_{1g}+1B_{2g}+2B_{1u}+1E_g+3E_u.$$

Each E vibration is twofold degenerate. Group theory reveals four distinct infrared frequencies: one of symmetry A_{2u}, and three of symmetry E_u. In addition, as discussed by Barker,[3] internal fields lift the degeneracies between the transverse and longitudinal infrared phonons. There are four Raman-active modes with symmetries A_{1g}, B_{1g}, B_{2g}, and E_g.

Corresponding to each Raman-active mode, there is a scattering tensor α having a distinctive symmetry. For the four allowed Raman transitions in materials of the D_{4h} point group these tensors have the form[11]

$$\alpha(A_{1g})=\begin{bmatrix} a & 0 & 0 \\ 0 & a & 0 \\ 0 & 0 & b \end{bmatrix},$$

$$\alpha(E_g)=\begin{bmatrix} 0 & 0 & 0 \\ 0 & 0 & d \\ 0 & d & 0 \end{bmatrix}, \quad \begin{bmatrix} 0 & 0 & d \\ 0 & 0 & 0 \\ d & 0 & 0 \end{bmatrix}$$

$$\alpha(B_{1g})=\begin{bmatrix} c & 0 & 0 \\ 0 & -c & 0 \\ 0 & 0 & 0 \end{bmatrix}, \quad \alpha(B_{2g})=\begin{bmatrix} 0 & e & 0 \\ e & 0 & 0 \\ 0 & 0 & 0 \end{bmatrix}.$$

To examine experimentally a given component α_{ij} one merely arranges the experimental geometry such that the incident light is polarized in the "i" direction while only that scattered light of "j" polarization is

[1] L. F. Johnson, R. E. Dietz, and H. J. Guggenheim, Phys. Rev. Letters **11**, 318 (1963).
[2] D. M. Eagels, J. Phys. Chem. Solids **25**, 1243 (1964).
[3] A. S. Barker, Jr., Phys. Rev. **136**, A1290 (1964).
[4] M. Balkunski, P. Moch, and G. Parisot, J. Chem. Phys. **44**, 940 (1966).
[5] B. Dayal, Proc. Indian Acad. Sci. **32A**, 304 (1950).
[6] P. S. Narayanan, Proc. Indian Acad. Sci. **37A**, 411 (1953).
[7] D. Krishnumarti, Proc. Indian Acad. Sci. **55A**, 290 (1962).
[8] R. S. Krishnan and R. S. Katiyar, J. Phys. Radium **26**, 627 (1965).
[9] R. S. Krishnan and J. P. Russell, British J. Appl. Phys. **17**, 501 (1966).
[10] P. S. Narayanan, Proc. Indian Acad. Sci. **32A**, 279 (1950).
[11] R. Loudon, Proc. Phys. Soc. (London) **82**, 393 (1963).

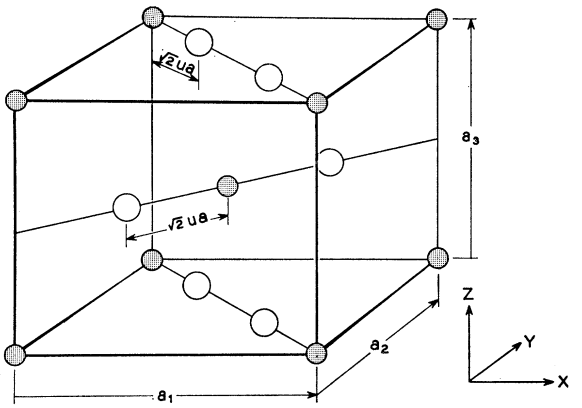

FIG. 1. Tetragonal unit cell for D_{4h} materials. Shaded and open circles represent positive and negative ions, respectively. $a_1=a_2=a$; $a_3=c\neq a$.

observed. For further details on experimental geometries see Ref. 12.

As the unit cell of Fig. 1 suggests, the crystals studied here are uniaxial. Thus, determination of the c axis (z direction) may be conveniently done optically as well as by the use of x rays. However, proper determination of the a axes (x-y plane orientation) is sometimes difficult. Improper sample orientation in the x-y plane complicates interpretation of Raman data. For a sample whose laboratory axes $x'y'$ are oriented at an angle θ with respect to the crystal x-y axes, the strengths of the α_{xx} and α_{xy} scatterings are multiplied by factors $(2\sin\theta\cos\theta)^2$ and $(\cos^2\theta-\sin^2\theta)^2$, respectively. We have verified this orientation dependence in a TiO_2 sample cut in the form of a cylinder about its c axis. As the sample was rotated the intensities of the B_{1g} and B_{2g} lines varied according to the above trigonometric expressions. Thus, for a D_{4h} crystal an error in x-y orientation can result in incorrect assignments of the B_{1g} and B_{2g} phonons. An additional consequence of improper orientation is the inability to discriminate against two-phonon processes on the basis of scattering tensor symmetries.

RESULTS AND DISCUSSION

The frequencies and symmetry assignments for the Raman-active phonons in the five materials studied here are summarized in Table I.

TABLE I. Raman-active phonons.

	TiO_2 (cm^{-1})	MgF_2 (cm^{-1})	ZnF_2 (cm^{-1})	FeF_2 (cm^{-1})	MnF_2 (cm^{-1})
B_{1g}	143	92	70	73	61
E_g	447	295	253	257	247
A_{1g}	612	410	350	340	341
B_{2g}	826	515	522	496	476

[12] T. C. Damen, S. P. S. Porto, and B. Tell, Phys. Rev. **142**, 570 (1966).

TABLE II. Infrared-active, transverse optical phonons.

	TiO_2[a] (cm^{-1})	MgF_2[b] (cm^{-1})	ZnF_2[b] (cm^{-1})	FeF_2[c] (cm^{-1})	MnF_2
E_u	183	247	173	200	···
E_u	388	410	244	320	···
E_u	500	450	380	480	···
A_{2u}	167	399	294	440	···

[a] Reference 2.
[b] Reference 3.
[c] Reference 4.

TABLE III. Longitudinal optical phonons.

	TiO_2[a] (cm^{-1})	MgF_2[b] (cm^{-1})	ZnF_2[b] (cm^{-1})	FeF_2	MnF_2
E_u	373	303	227	···	···
E_u	458	415	264	···	···
E_u	806	617	498	···	···
A_{2u}	811	625	488	···	···

[a] Reference 2.
[b] Reference 3.

For completeness, Tables II and III summarize the previously reported results of infrared experiments, where available, by other workers. We shall discuss

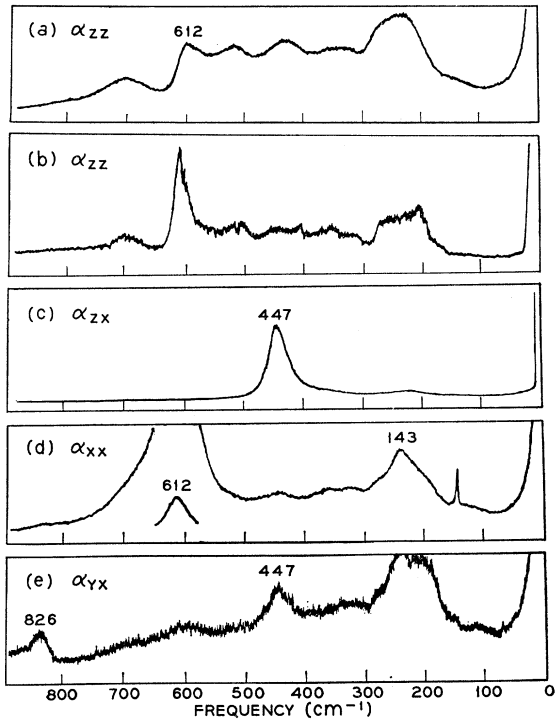

FIG. 2. Raman spectrum of TiO_2; instrumental width ~1.5 cm^{-1}. (a) α_{zz} component showing strong combination bands. The α_{zz} component of the A_{1g} phonon, 612 cm^{-1}, is obscured by two-phonon processes at room temperature, but dominates at 77°K. (b) α_{zz} component taken at liquid-nitrogen temperature, showing clearly the emergence of the 612-cm^{-1} line as a fundamental above the neighboring combination bands. All other spectra exhibited in this paper were obtained at room temperature. (c) α_{zx} component showing phonon of E_g symmetry at 447 cm^{-1}. (d) α_{xx} component showing B_{1g} and A_{1g} phonons at 143 and 612 cm^{-1}, respectively, as well as very strong two-phonon bands. (e) α_{yx} component showing the B_{2g} phonon at 826 cm^{-1} and two-phonon bands.

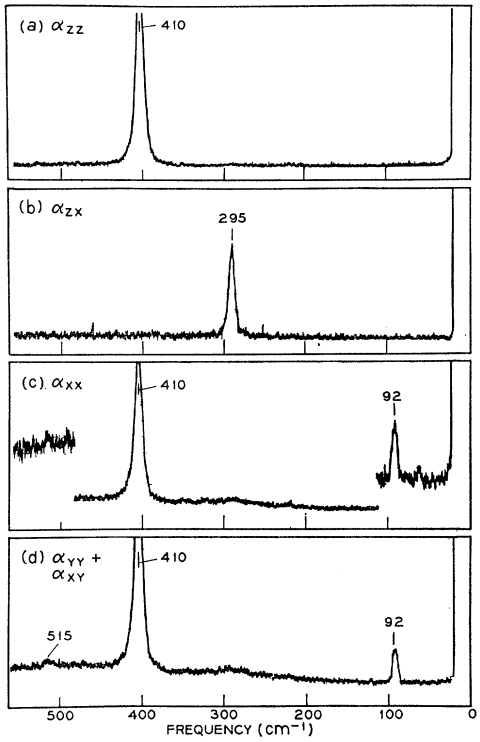

FIG. 3. Raman spectrum of MgF_2; instrumental width $\sim$3 cm^{-1}. (a) α_{zz} component showing A_{1g} phonon at 410 cm^{-1}. (b) α_{zx} component showing E_g phonon at 295 cm^{-1}. (c) α_{xx} component showing B_{1g} and A_{1g} phonons at 92 and 410 cm^{-1}, respectively. Gain increase by a factor of 10 shows clearly the B_{1g} phonon. (d) α_{yy} and α_{xy} components together showing B_{1g} and A_{1g} again. Notice the small peak at 515 cm^{-1} which is due to the B_{2g} phonon.

each material in turn in the light of the observed Raman spectra (see Figs. 2–6).

(*a*) *TiO_2*. Though several authors[5–7] have reported observation of the Raman effect in TiO_2, there has not been agreement among them as to phonon frequencies and symmetries. In large measure, these disagreements arise from the relatively strong two-phonon processes in TiO_2. Without careful polarization studies, the clear-cut symmetries associated with fundamental (one-phonon) processes cannot be exploited. For example, Fig. 2 shows a strong band at $\sim$235 cm^{-1} in TiO_2, which under high resolution exhibits considerable structure. Largely because of its strength, several workers have assigned this band to a fundamental process.[5,9] Detailed examination of the scattering tensor associated with the 235-cm^{-1} peak, however, does not reveal a simple symmetry corresponding to any of the one-phonon Raman tensors displayed in Sec. II. This peak exhibits nonzero tensor elements α_{xx}, α_{yy}, α_{zz}, and α_{xz}; and is therefore a combination line. Further, from the room-temperature spectrum in Fig. 2(a), the 612-cm^{-1} phonon is nearly obscured by combination bands. However, Fig. 2(b), taken at liquid-nitrogen temperature, shows clearly the 612-cm^{-1} line as a fundamental process. This observation is complemented by the room-temperature α_{xx} spectrum, Fig. 2(d), which completes identification of the 612-cm^{-1} line as A_{1g}. The sharp B_{1g} phonon at 143 cm^{-1} and the weak B_{2g} phonon at 826 cm^{-1} are evident in the α_{xx} and α_{yx} spectra, respectively. The E_g phonon is clearly identified in Fig. 2(c) at 447 cm^{-1}.

(*b*) *MgF_2*. The recent reports of Raman studies in MgF_2 by Krishnan and Katiyar[8] and by Krishnan and Russell[9] are in disagreement with each other and with our results. First, the line at 72 cm^{-1} reported in Refs. 8 and 9 and identified as B_{1g} and B_g, respectively, is not observed by us. This is clearly shown in Fig. 3. (The notation B_g is employed by Krishnan and Russell to indicate the inability to distinguish between B_{1g} and

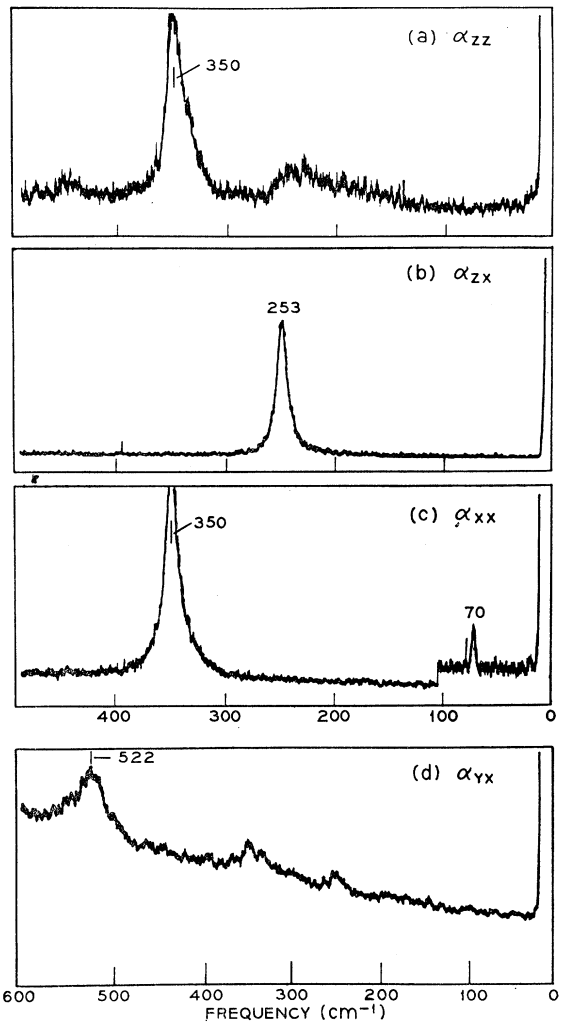

FIG. 4. Raman spectrum of ZnF_2; instrumental width $\sim$3 cm^{-1}. (a) α_{zz} component showing the A_{1g} phonon at 350 cm^{-1} and two-phonon bands. (b) α_{zx} component showing the E_g phonon at 253 cm^{-1}. (c) α_{xx} component showing the B_{1g} and A_{1g} phonons at 70 and 350 cm^{-1}, respectively. A factor of 3 increase in gain shows clearly the B_{1g} phonon. (d) α_{yx} component showing the B_{2g} phonon at 522 cm^{-1} superimposed on the tail of a weak fluorescence band. A small amount of leakage of the A_{1g} and E_g phonon lines is evident.

B_{2g} in their experiment.) Instead, we identify as the B_{1g} phonon the 92-cm^{-1} line clearly visible in the figure. This line was also observed by Krishnan and Katiyar but was ignored in their analysis. Another line reported at ~155 cm^{-1} and identified as E_g and B_g in Refs. 8 and 9, respectively, was not observed by us. Figure 4 shows clearly that the line whose symmetry is E_g has a frequency of 295 cm^{-1}, while the A_{1g} phonon is at 410 cm^{-1}. The B_{2g} line we observe at 515 cm^{-1} is extremely weak, as are the B_{2g} lines for all of the D_{4h} crystals studied. However, the symmetry of the scattering tensor is that expected for the B_{2g} vibration.

(*c*) *ZnF_2*. As indicated in the tables above, ZnF_2 has been thoroughly studied in the infrared by Barker.[3] We find that the frequencies and symmetry assignments for the Raman-active phonons follow the same general pattern as those discussed above in TiO_2 and MgF_2. The Raman spectra are displayed in Fig. 4 where it is clear that the lines at 70, 253, 350, and 522 cm^{-1} are due

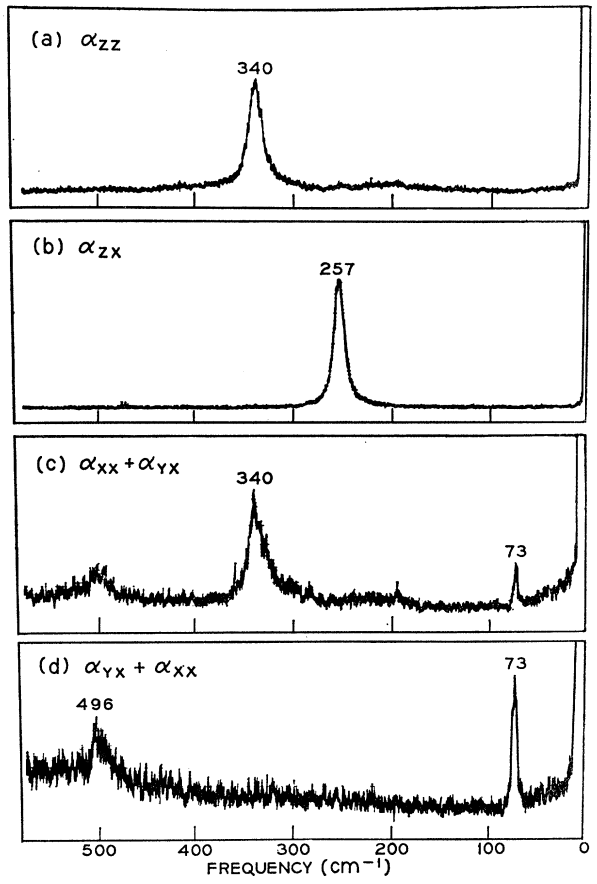

FIG. 5. Raman spectrum of FeF_2; instrumental width ~3 cm^{-1}. The sample was misoriented in the *x-y* plane by 19°. (a) α_{zz} component showing the A_{1g} phonon at 340 cm^{-1}. (b) α_{zx} component showing the E_g phonon at 257 cm^{-1}. (c) α_{xx} component with a small leakage of α_{yx} due to 19° misorientation. Thus the B_{1g} and A_{1g} phonons at 73 and 340 cm^{-1}, respectively, appear together with the weak B_{2g} phonon at 496 cm^{-1}. (d) α_{yx} component with small amount of α_{xx} component. The B_{1g} and B_{2g} phonons at 73 and 496 cm^{-1} are evident.

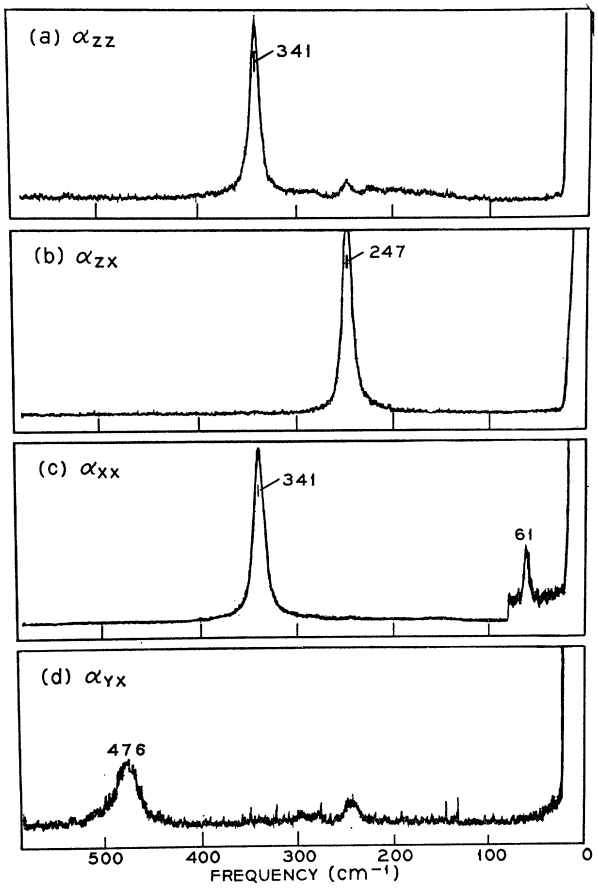

FIG. 6. Raman spectrum of MnF_2; instrumental width ~3 cm^{-1}. (a) α_{zz} component showing the A_{1g} phonon at 341 cm^{-1} and a very weak two-phonon band. (b) α_{zx} component showing the E_g phonon at 247 cm^{-1}. (c) α_{xx} component showing the A_{1g} and B_{1g} phonons at 341 and 61 cm^{-1}, respectively. The gain is increased by a factor of 10 to show the B_{1g} phonon clearly. (d) α_{yx} component showing the B_{2g} phonon at 476 cm^{-1} and a leakage of the much stronger E_g phonon.

to phonons with symmetries B_{1g}, E_g, A_{1g}, and B_{2g}, respectively. In this case the B_{2g} phonon is clearly visible above the noise.

(*d*) *FeF_2 and MnF_2*. Figures 5 and 6 reveal the Raman spectra of FeF_2 and MnF_2 to be quite similar to those already discussed. Additional interest arises in these cases, however, because these materials become antiferromagnetic at low temperatures (T_N=67.7°K for MnF_2; 78.5°K for FeF_2). The magnons in the magnetic state have been studied in both optical[13] and infrared absorption[14] experiments, as well as by light scattering.[15] In FeF_2 [15] the magnon frequency increases from 53 cm^{-1} at the center of the Brillouin zone to ~77 cm^{-1} at the

[13] R. L. Green, D. D. Sell, W. M. Yen, A. L. Schawlow, and R. M. White, Phys. Rev. Letters **15**, 656 (1965) and references cited therein.

[14] S. J. Allen, R. Loudon, and P. L. Richards, Phys. Rev. Letters **16**, 463 (1966), and references cited therein.

[15] P. A. Fleury, S. P. S. Porto, L. E. Cheesman, and H. J. Guggenheim, Phys. Rev. Letters **17**, 84 (1966).

zone edge. The low-frequency B_{1g} phonon we have observed at 73 cm^{-1} in FeF_2 may possibly interact with the magnon away from the center of the zone. In MnF_2[15] a similar situation exists: The magnon frequency increases from $\sim$8.5 cm^{-1} to $\sim$56 cm^{-1} from zone center to zone edge; and the B_{1g} phonon frequency is 61 cm^{-1}. Of course, the phonon frequencies given here are room-temperature values, while the magnon frequencies were obtained at low ($<20°K$) temperatures. Some frequency shift with temperature will occur in the phonons, and some dispersion in phonon frequency will occur in going from the zone center to the zone boundary. Nevertheless, neither of these effects should be large enough to eliminate completely the possibility of phonon-magnon interaction in these materials. In fact, measurements of the zone-center B_{1g} phonon frequencies at $\sim 20°K$ reveal $\sim$71 cm^{-1} and $\sim$57 cm^{-1} for FeF_2 and MnF_2, respectively.

Finally, some comments on the general features of the phonons in the D_{4h} compounds are in order. Matossi[16] has proposed a model for the vibrational modes in the rutile structure based on seven force constants and the masses and bond angles of the atoms involved. We present a few of his results in order to assess the validity of his model. Two results of Matossi are expressed in Eqs. (1) and (2):

$$\omega_2^2=\omega_4^2+\omega_3^2-\omega_1^2, \tag{1}$$

$$\omega_2^2=\omega_3^2\left(\frac{\cos\psi+\sin\psi}{\cos\psi-\sin\psi}\right)^2. \tag{2}$$

Here ω_1 is the A_{1g} phonon frequency; ω_2 is A_{2g}; ω_3 is B_{1g}; and ω_4 is B_{2g}. All but the A_{2g} frequency are measured in the Raman effect. The A_{2g} phonon is neither Raman nor infrared active. The angle ψ is defined by Matossi[16] and depends only on the lattice parameters of the solid. Equations (1) and (2) together with our measurements of ω_1, ω_3, and ω_4 provide a test of Matossi's model. Our Raman data and Eq. (1) yield A_{2g} frequencies ω_2 of 653, 326, 394, 368, and 338 cm^{-1} for TiO_2, MgF_2, ZnF_2, FeF_2, and MnF_2, respectively. Using values of ψ computed from measured lattice parameters,[17] together with Eq. (2), results in values for ω_2 of 686, 434, 335, 361, and 282 cm^{-1}, respectively. With regard to this simple test of internal consistency, Matossi's model is moderately successful—the maximum discrepancy being $\sim$30% in the case of MgF_2. However, agreement between calculations and experiment is much poorer in the case of some infrared phonons, particularly A_{2u}. Such discrepancies have discouraged us from including any values for the B_{2u} phonon frequencies calculated from Matossi's model. Since both infrared and Raman data are now available on several of the D_{4h} materials, a re-examination of their lattice dynamics seems in order.

SUMMARY

The first-order Raman effect has been measured at room temperature in the crystals of D_{4h} symmetry: TiO_2, MgF_2, ZnF_2, FeF_2, and MnF_2. The four Raman-active phonons predicted by group theory were found for each crystal. Each spectrum exhibits strong lines of A_{1g} and E_g symmetries, a sharp low-frequency line of B_{1g} symmetry, and a weak high-frequency line of B_{2g} symmetry. The somewhat richer structure of the TiO_2 spectra is due to large second-order Raman effect, not evident in the fluorides studied.

ACKNOWLEDGMENTS

We thank A. Albert and V. C. Wade for assistance with sample preparation and H. J. Guggenheim for providing the MnF_2 and FeF_2.

[16] F. Matossi, J. Chem. Phys. **19**, 1543 (1951).

[17] R. W. G. Wycoff, *Crystal Structures* (Interscience Publishers, Inc., New York, 1960), Vol. 1, p. 251.